MASTER THESIS

A New Algorithm of Analyzing the Anderson Localization

Junko Yamasaki

Department of Physics,
Graduate College of Science and Engineering,
Aoyama Gakuin University

Supervisor: Naomichi Hatano

2001

論　文　要　旨
（和　文）

提 出 年 度： 2001 年度
提　出　日： 2002 年 2 月 23 日
専　　攻： 物理学専攻
学 生 番 号： 35100024
学 生 氏 名： 山崎 淳子
研究指導教員：羽田野 直道

（論文題目）

非エルミートハミルトニアンを用いたアンダーソン局在の研究

（内容の要旨）

金属中の不純物濃度が増加すると、金属は金属－絶縁体転移を起こす。この転移をアンダーソン局在という。本研究の目的は金属－絶縁体転移を数値解析することである。

研究には 1 次元のアンダーソンモデルを用いた。このモデルはランダムポテンシャル中の 1 電子の運動を表す。局在する波動関数は一般的に$\psi(\vec{x}) \sim \exp(-\alpha |\vec{x} - \vec{x}_0|)$の形に書ける。このとき、局在長は波動関数の中心$\vec{x}_0$から$\alpha^{-1}$の広がりを持っているといえる。$\alpha = 0$のとき電子は非局在状態で金属状態である。$\alpha > 0$のとき電子は局在状態で絶縁体の状態である。我々が計算したいのは局在長α^{-1}である。

1 電子アンダーソンモデルの局在長の新しい計算法を Hatano と Nelson が提案した。それは、運動量の項に虚数ベクトルポテンシャルを加えて非エルミート化したハミルトニアンを対角化し、複素エネルギースペクトルを調べるという方法である。これまでの方法では波動関数から局在長を求めていたが、この新しい方法では、非エルミート行列のエネルギースペクトルを求めるだけで局在長を得ることができる。

しかし、実際の数値計算で大きな非エルミート行列を対角化することは困難である。そこで本研究では、非エルミート行列の固有値を計算するかわりに擬スペクトルを計算する方法を提案し、その結果を示す。擬スペクトルは非エルミート行列の最小特異値のz平面上の等高線である。その等高線が非エルミート行列のスペクトルを近似する。擬スペクトルの計算には大きいエルミート行列の固有値を求めるのに有用なランチョス法を用いることができる。ランチョス法は並列化をすることも可能なので大きな系の計算が期待される。

Academic Year of 2001, Submitted on Feb. 23 , 2002

Graduate College of Science and Engineering, Aoyama Gakuin University

Master Thesis

A new algorithm of analyzing the Anderson localization

Junko Yamasaki (35100024)
Supervisor : Naomichi Hatano
Department of Physics

Abstruct

Upon increasing the impurity concentration, a metal undergoes a phase transition to an insulator owing to the Anderson localization. The aim of the present study is to analyze the metal-insulator transition numerically, using the one-electron Anderson models in a random potential and a random flux. When a wave function of the model has the form: $\psi(\vec{x}) \sim \exp(-\kappa |\vec{x} - \vec{x}_0|)$, its localization length around the localization center $\vec{x}_0$ is given by κ^{-1}. The electron is delocalized if $\kappa = 0$ and hence represents a metal, whereas it is localized if $\kappa > 0$ and represents an insulator. Our purpose is to compute the energy dependence of κ^{-1} for a given random potential.

Recently Hatano and Nelson suggested a new numerical algorithm of computing the localization length κ^{-1}. The algorithm is to generalize the conventional Hermitian Hamiltonian to a non-Hermitian Hamiltonian with an imaginary vector potential g in the kinetic term of the Hamiltonian. We can obtain the localization length by computing the eigenvalue spectrum of the non-Hermitian Hamiltonian. In the conventional method, κ^{-1} is calculated only after computing the wave function $\psi(\vec{x}) \sim \exp(-\kappa |\vec{x} - \vec{x}_0|)$. In the new method, we compute only the eigenvalues of the non-Hermitian Hamiltonian.

Unfortunately, it is difficult to diagonalize large non-Hermitian matrices.
Thus we propose a new algorithm. We compute the pseudo-spectrum instead of computing the energy spectrum. The pseudo-spectrum is a contour plot of the minimum singular value of a non-Hermitian matrix $(z - H)$ in the complex plain. The pseudo-spectrum approximates the energy spectrum of the non-Hermitian matrix. This method is suitable for treating huge sparse matrices; the code can be fully parallelized.

We applied the new algorithm to non-Hermitian Anderson models in a random potential and in a random magnetic field. The results suggest the need of a fine tuning of the convergence parameter.

MASTER THESIS
A new algorithm of analyzing the Anderson localization

Junko Yamasaki
Department of Physics, Aoyama Gakuin University
Chitosedai, Setagaya, Tokyo 157-8572, Japan

March 26, 2002

Abstract

Upon increasing the impurity concentration, a metal undergoes a phase transition to an insulator owing to the Anderson localization. The aim of the present study is to analyze the metal-insulator transition numerically, using the one-electron Anderson models in a random potential and in a random flux. When a wave function of the model has the form $\psi(\vec{x}) \sim e^{-\kappa|\vec{x}-\vec{x}_0|}$, its localization length around the localization center $\vec{x}_0$ is given by κ^{-1}. The electron is delocalized if $\kappa = 0$ and hence represents a metal, whereas it is localized if $\kappa > 0$ and represents an insulator.

Our purpose is to compute the energy dependence of κ^{-1} for a given random potential. Recently Hatano and Nelson suggested a new numerical algorithm of computing the localization length κ^{-1} . The algorithm is to generalize the conventional Hermitian Hamiltonian to a non-Hermitian Hamiltonian with an imaginary vector potential g in the kinetic term of the Hamiltonian. We can obtain the localization length by computing the eigenvalue spectrum of the non-Hermitian Hamiltonian. In the conventional method, κ^{-1} is calculated only after computing the wave function $\psi(\vec{x}) \sim e^{-\kappa|\vec{x}-\vec{x}_0|}$. In the new method, we compute only the eigenvalues of the non-Hermitian Hamiltonian.

Unfortunately, it is difficult to diagonalize large non-Hermitian matrices. Thus we propose a new algorithm. We compute the pseudospectrum instead of computing the energy spectrum. The pseudospectrum is a contour plot of the minimum singular value of a non-Hermitian matrix in the complex plain. The pseudospectrum approximates the energy spectrum of the non-Hermitian matrix. This method is suitable for treating huge sparse matrices; the code can be fully parallelized. We applied the new algorithm to non-Hermitian Anderson models in a random potential and in a random magnetic field. The results suggest the need of a fine tuning of the convergence parameter.

Contents

1 Introduction

Upon increasing the impurity concentrarion, a metal undergoes a phase transition to an insulator owing to the Anderson localization. The aim of the present study is to analyze the metal-insulator transition numerically. We use the one-electron Anderson model

$$H = \frac{\vec{p}^2}{2m} + V(\vec{x}) = -\frac{\hbar^2}{2m}\vec{\nabla}^2 + V(\vec{x}), \tag{1}$$

where $\vec{p} = (\hbar/i)\partial/\partial x$ is the momentum operator and $V(\vec{x})$ is a random potential. By solving the Schrödinger equation for the Hamiltonian (1), we may have a wave function of the form

$$\psi(\vec{x}) \sim e^{-\kappa|\vec{x}-\vec{x}_0|}. \tag{2}$$

Then its localization length around the localization center $\vec{x}_0$ is given by κ^{-1}. The electron is delocalized if $\kappa = 0$ and hence represents a metal, whereas it is localized if $\kappa > 0$ and represents an insulator. Our purpose is to compute the energy dependence of κ for a given random potential $V(\vec{x})$.

In the present thesis, we develop a new numerical algorithm of computing the inverse localization length κ. In Sec.2, we review a method of obtaining the localization length using a non-Hermitian Hamiltonian. In Sec.3, we investigate the eigenspectrum of the ladder Anderson models in an imaginary vector potential. In Sec.4, we introduce our new algorithm of computing an aproximate eigenspectrum of non-Hermitian matrices, from which we wish to estimate the localization length κ of the Hermitian Anderson model.

2 Non-Hermitian Hamiltonian and Computation of the Localization Length

In the present section, we review a recently introduced method of estimating the localization length of the Anderson model. We also show a numerical example for the one-dimensional lattice Anderson model.

2.1 Imaginary Vector Potential

It was recently shown [1, 2] that the eigenvalue spectrum of the non-Hermitian generalization of (1),

$$\begin{aligned} H &= \frac{(\vec{p}+i\vec{g})^2}{2m} + V(\vec{x}) \\ &= -\frac{1}{2m}(\hbar\vec{\nabla} - \vec{g})^2 + V(\vec{x}) \end{aligned} \tag{3}$$

yields κ of the Hermitian Hamiltonian (1). Here we refer to the field $\vec{g}$ as the imaginary vector potential. This method of computing the localization length is of recent interest as a very different method from the conventional one; In the conventional method, the inverse localization κ is calculated directly from (2) after computing the wave function.

Let us review the new method briefly. Consider first an eigenstate $\psi_0(\vec{x})$ for $\vec{g} = \vec{0}$. The Hamiltonian in this case is Hermitian, and hence the corresponding eigenvalue ε_0 is real. Focusing on this particular state, we switch on the imaginary vector potential $\vec{g}$ and gradually increase it. The following three properties were shown [1, 2]:

1. There is a critical point $|\vec{g}| = g_c$, where the eigenstate gets delocalized in a novel, non-Hermitian way;

2. The value of the critical point g_c is equal to $\hbar\kappa$ of the Hermitian Anderson model (1);

3. Below the critical point, the corresponding eigenvalue is fixed to ε_0, while above it, the eigenvalue is generally complex and dependent on the imaginary vector potential $\vec{g}$.

Using these properties, we can estimate κ from g_c, when the eigenvalue begins to move in the complex energy plane. We explain in this section the above properties and the method of calculating κ.

2.2 Non-Hermitian Gauge transformation

In order to show the above three properties, we use the gauge transformation. Suppose that we solve the eigenvalue problem without the imaginary vector potential and obtain the wave function

$$\psi(\vec{x};0) \sim e^{-\kappa|\vec{x}|}. \tag{4}$$

Now we introduce a constant imaginary vector potential $\vec{g}$. If it were a usual, real vector potential $\vec{A}$, we should be able to gauge it out. That is, the eigenfunction is given by

$$\psi(\vec{x};\vec{A}) = e^{i\frac{\vec{A}}{\hbar}\cdot\vec{x}}\psi(\vec{x};0) \tag{5}$$

and the eigenvalue remains the same:

$$\varepsilon(\vec{A}) = \varepsilon(0). \tag{6}$$

Applying the same argument, the eigenfunction for the imaginary vector potential may be given by

$$\psi(\vec{x};\vec{g}) = e^{\frac{\vec{g}}{\hbar}\cdot\vec{x}}\psi(\vec{x};0) \sim e^{\frac{\vec{g}}{\hbar}\cdot\vec{x}-\kappa|\vec{x}|}, \tag{7}$$

whereas the eigenvalue may remain the same and is a real number,

$$\varepsilon(\vec{g}) = \varepsilon(0) \tag{8}$$

For $g = |\vec{g}| > \hbar\kappa$, however, the function (7) is diverging and cannot be an eigenfunction. Thus the eigenfunction changes and the eigenvalue generally becomes complex.

When $g = 0$, all eigenvalues are real because the Hamiltonian is Hermitian. As we increase g, the eigenfunction gets delocalized at a certain point g_c, which is equal to $\hbar\kappa$ as can be seen in (7). The relation between the eigenvalue and the eigenfunction is:

1. The eigenfunction is localized if its eigenvalue is a real number;

2. The eigenfunction is delocalized if its eigenvalue is a complex number.

Thus, the change of the eigenvalue from real to complex indicates the critical point g_c, from which we can estimate the inverse localization length κ of the original eigenfunction. In other words, We can know how strongly the engenfunction was localized at the beginning by measuring the critical value g_c.

2.3 One-dimentional lattice model

We here show a numerical example [1] by using a one-dimensional lattice version of the non-Hermitian Hamiltonian (3). The Hamiltonian is given by [1, 2]

$$H = \sum_{x=1}^{L} \left[\frac{t}{2} \Big(e^{gx} \left| x + a \right\rangle \left\langle x \right| + e^{-gx} \left| x \right\rangle \left\langle x + a \right| \Big) + V_x \right], \tag{9}$$

where g is again the imaginary vector potential, a is the lattice constant, and V_x is a site random potential with a box distribution in the range $[-t, t]$. The complex energy spectrum is shown in Fig. 1. Using the above method, we can evaluate the energy dependence of the inverse localization length κ as in Fig. 2.

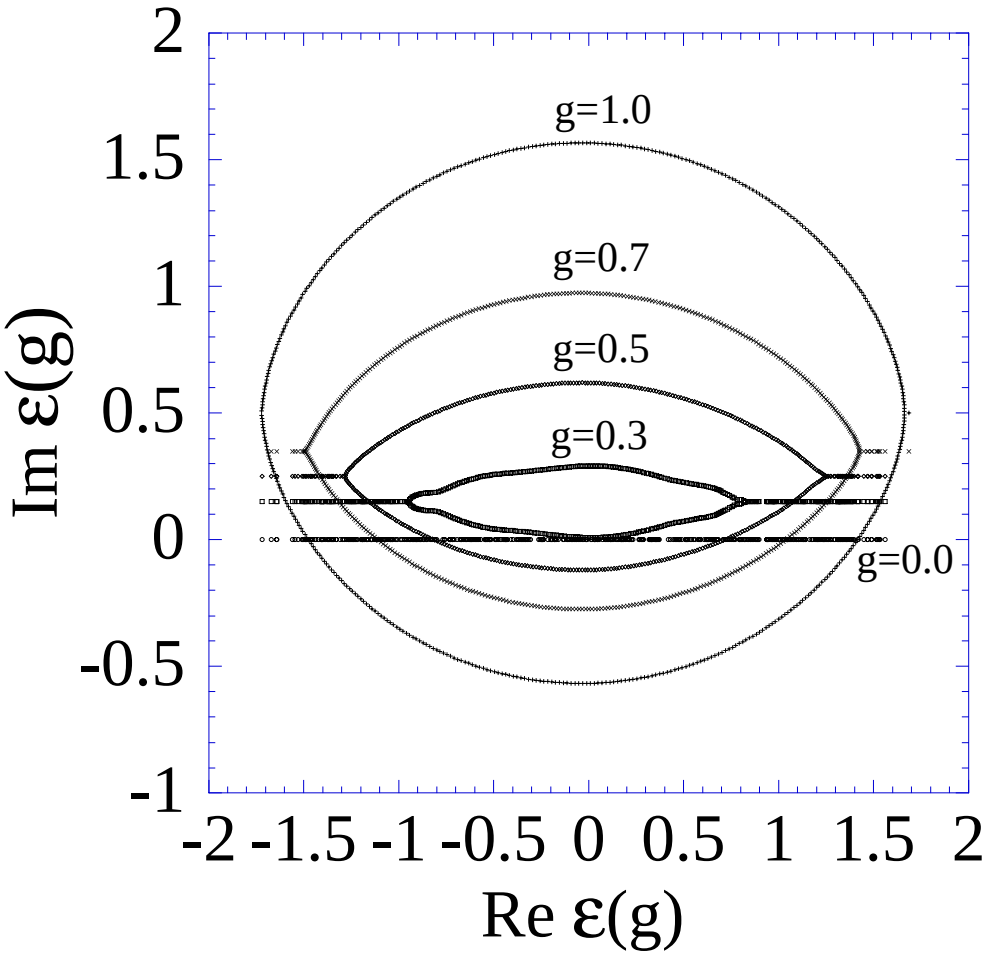

Figure 1: The complex energy spectrum of the Hamiltonian (9) for various values of the imaginary vector potential g. The system size is $L = 500$. Each symbol indicates an eigenvalue. For explanatory purposes, we shifted the real axis upwards for $g > 0$.

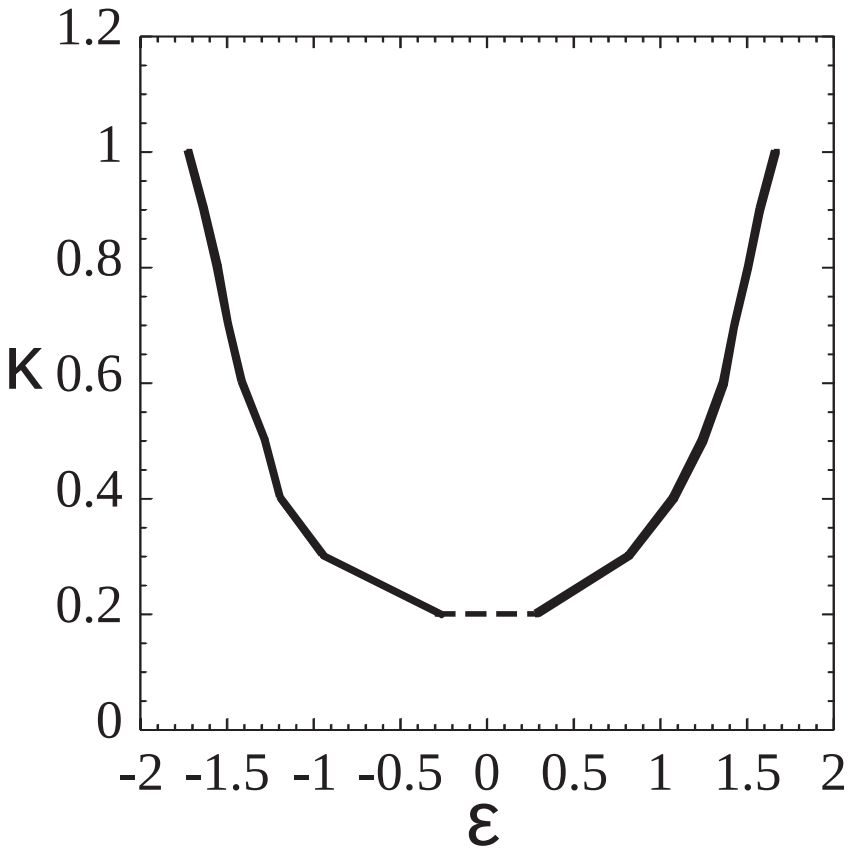

Figure 2: The energy dependence of the inverse localization length κ of the one-dimensional Hermitian Anderson model (9) with $g = 0$. The result is obtained from the data in Fig. 1.

3 Ladder Anderson Models

In the present section, we define the ladder Anderson model in a random on-site potential and that in a random magnetic flux. In light of the method of estimating the localization length reviewed in Sec. 2, we investigate the eigenspectrum of the ladder models with an imaginary vector potential. These models show interesting features of the eigenvalues.

3.1 Ladder Model in a Random On-Site Potential

We analyze a ladder model in a random on-site potential, given by

$$H_V(g) = \sum_{i=1}^{N_{\rm leg}} H_i + \sum_{i=1}^{N_{\rm leg}-1} H_{i,i+1}, \tag{10}$$

where H_i is the non-Hermitian Anderson Hamiltonian for the leg i of the ladder,

$$H_i = \sum_{x=1}^{L} \left[\frac{t}{2} \Big(e^{gx} \left| x;i \right\rangle \left\langle x+1;i \right| + e^{-gx} \left| x+1;i \right\rangle \left\langle x;i \right| \Big) + V_x \right], \tag{11}$$

while $H_{i,i+1}$ is the hopping term between the two legs i and $i+1$,

$$H_{i,i+1} = \sum_{x=1}^{L} \left[\frac{t}{2} \Big(\left| x;i+1 \right\rangle \left\langle x;i \right| + \left| x;i \right\rangle \left\langle x;i+1 \right| \Big) \right]. \tag{12}$$

We make V_x random with a box distribution in the range $[-t, t]$. Note that the imaginary vector potential g is included in (11) only.

We computed numerically the complex energy spectrum of the Hamiltonian of the Hamiltonian (10) by the Householder method. Each spectrum in Fig 3 is composed of $N_{\rm leg}$ branches of similar sizes shifted horizontally. This means that the Hermitian limit of the ladder Anderson model has several branches of $\kappa(\varepsilon)$ shifted holizontally with each branch similar to the one in Fig.1.

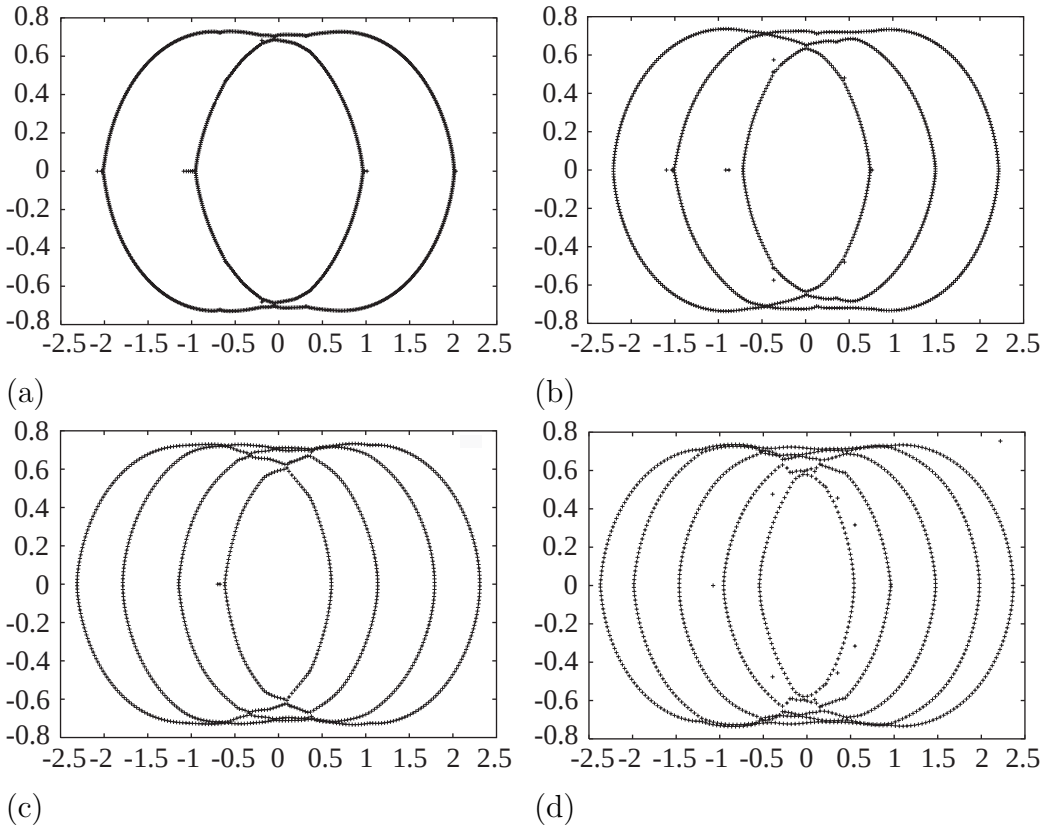

Figure 3: The energy spectrum of the ladder model in a random on-site potential of the Hamiltonian (10) for $g = 0.8$: (a) The number of legs $N_{\rm leg} = 2$, $L = 500$; (b) $N_{\rm leg} = 3$, $L = 300$; (c) $N_{\rm leg} = 4$, $L = 250$; (d) $N_{\rm legs} = 5$, $L = 200$.

3.2 Ladder Model in a Random Magnetic Field

The Anderson localization was originally considerd as problems in a random on-site potential. We can extend the argument to problems in random magnetic fields.

The magnetic field $\vec{B}$ is related to the vector potential $\vec{A}$ as

$$\vec{B} = \mathrm{rot}\, \vec{A}. \tag{13}$$

A random magnetic field is thus genereted by a random vector potential. In the present paper, we analyze a ladder model with a random vector potential, given by

$$H_A(g) = \sum_{i=1}^{N_{\mathrm{leg}}} H_i + \sum_{i=1}^{N_{\mathrm{leg}}-1} H_{i,i+1}, \tag{14}$$

where H_i is the non-Hermitian Anderson Hamiltonian for the leg i of the ladder,

$$H_i = \sum_{x=1}^{L} \left[\frac{t}{2} \Big(e^{(iA_{x;i}+g)x} \left|x;i\right\rangle \left\langle x+1;i\right| + e^{-(iA_{x;i}+g)x} \left|x+1;i\right\rangle \left\langle x;i\right| \Big) \right], \tag{15}$$

while $H_{i,i+1}$ is the hopping term between the two legs i and $i+1$,

$$H_{i,i+1} = \sum_{x=1}^{L} \left[\frac{t}{2} \Big(e^{iA_{x;i,i+1}x} \left|x;i+1\right\rangle \left\langle x;i\right| + e^{-iA_{x;i,i+1}x} \left|x;i\right\rangle \left\langle x;i+1\right| \Big) \right]. \tag{16}$$

Here $A_{x;i}$ is a vector potential on the leg i and $A_{x;i,i+1}$ is a vector potential between the legs i and $i+1$. We make them random with a box distribution in the range $[-\pi, \pi]$. Note that the imaginary vector potential g is included in (15) only.

We also computed the complex energy spectrum of the Hamiltonian (14) numerically by the Householder method. See Figs. 4 and 5. In contrast to Fig. 3, each spectrum is composed of N_{leg} shells of different sizes but of the same center. This means that the Hermitian limit of the ladder Anderson model (14) has several branches of $\kappa(\varepsilon)$, each of which is similar to the one in Fig. 2 but with a different band width.

It was recently suggested that the nature of the localization is different from the ladders with even number of legs to those with odd number of legs. We wish to check the difference between odd and even legs. However, the tractable system size becomes small as the number of legs are increased. As

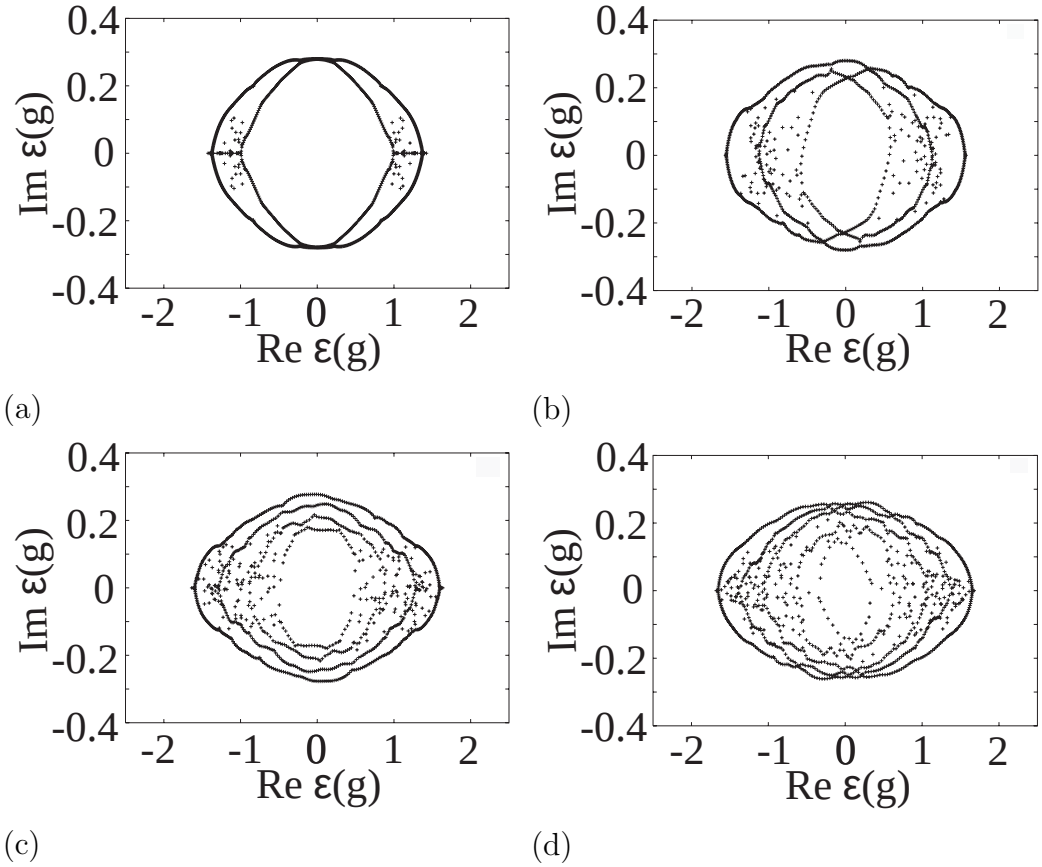

Figure 4: The energy spectrum of the ladder model in a random magnetic field of the Hamiltonian (14) for $g = 0.4$: (a) The number of legs $N_{\rm leg} = 2$, $L = 500$; (b) $N_{\rm leg} = 3$, $L = 300$; (c) $N_{\rm leg} = 4$, $L = 250$; (d) $N_{\rm leg} = 5$, $L = 200$.

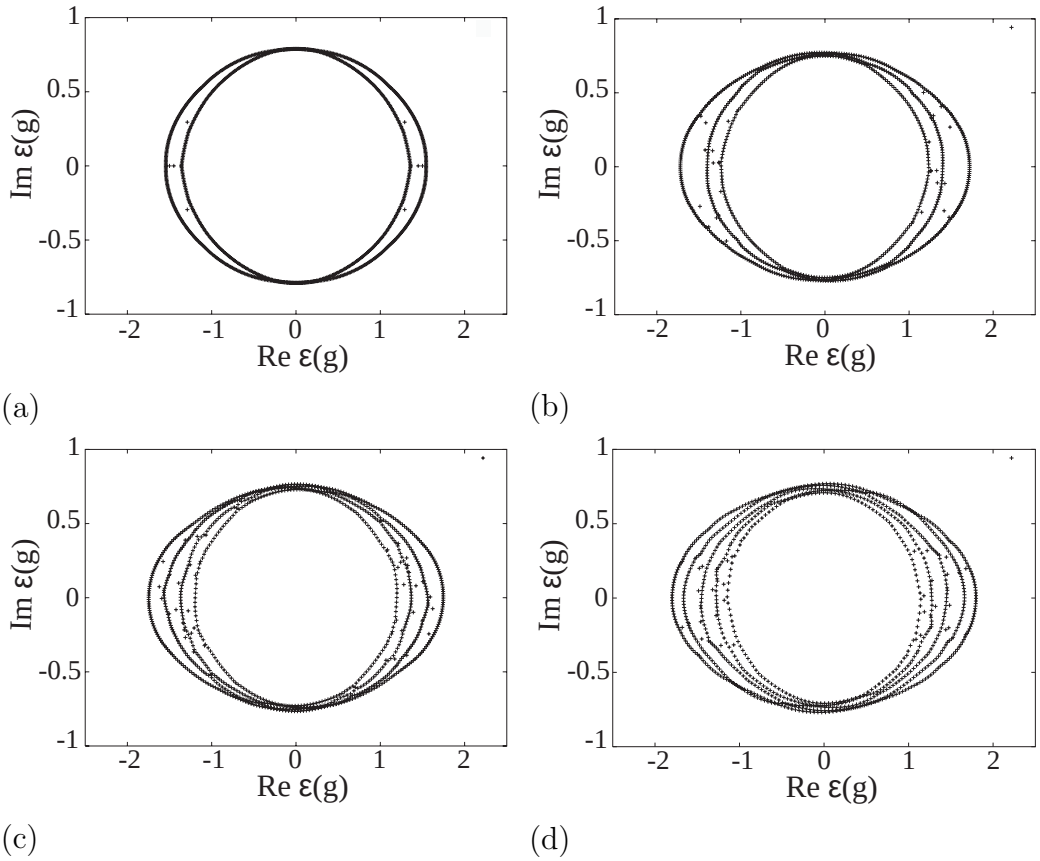

Figure 5: The energy spectrum of the ladder model in a random magnetic field of the Hamiltonian (14) for $g = 0.8$: (a) Number of legs $N_{\text{leg}} = 2$, $L = 500$; (b) $N_{\text{leg}} = 3$, $L = 300$; (c) $N_{\text{leg}} = 4$, $L = 250$; (d) $N_{\text{leg}} = 5$, $L = 200$.

far as we use the Householder algorithm to diagonalize the non-Hermitian Hamiltonians, the maximum ladder length L that we can treat is around 200 for $N_{\rm leg} = 5$. The spectrum becomes fuzzy as L decreases and it is hard to investigate the even-odd difference. This is one of our motivations of developing a new algorithm for large non-Hermiatian matrices, which we introduce in the next section.

4 Pseudospectrum of Non-Hermitian Models

The non-Hermitian method of computing the localization length, explained in Sec. 2, involves diagonalizing the non-Hermitian matrices (9), (10) and (14). In Figs. 1, 3, 4 and 5, we used the Householder method for the diagonalization of the asymmetric matrices [1]. Unfortunately, it is not an easy task to compute the eigenvalue spectrum of larger non-Hermitian matrices. The Householder method needs the working area of the order of N^2, where N is the matrix dimension. The Lanczos method, an efficient $O(N)$ method for sparse Hermitian matrices, is generally unstable for non-Hermitian matrices. To resolve this dilemma is the main point of the present section.

4.1 Pseudospectrum

Trefthen [3, 4] recently pointed out that the so-called pseudospectrum of the Hamiltonian matrix (9) is more suitable for the study of localization than the spectrum. There are several equivalent definitions of the pseudospectrum. One that can be physically interpreted is the following [4]:

> Definition 1: For any $\varepsilon \geq 0$, the ε-pseudospectrum $\Lambda_\varepsilon(H)$ of a matrix H is the set of the eigenvalues $z \in \mathbf{C}$ of $H + \Delta$ for some matrix Δ with $||\Delta|| \leq \varepsilon$.

In other words, the pseudospectrum is the spectrum of the matrix H with a small perturbation Δ. This reminds us of a well-known criterion of localized and delocalized states. According to Thouless [5, 6, 7], one can determine whether a state is localized or not by inspecting its sensitivity to the boundary conditions: If the eigenvalue of the state is sensitive to a twist of the boundary conditions, it is a delocalized state; If insensitive, it is a localized state. The above definition of the pseudospectrum is a quantification (and generalization) of the Thouless criterion. Trefthen demonstrated that, although every state of a Hermitian Hamiltonian has a real eigenvalue, some eigenvalues of a slightly perturbed Hamiltonian may be complex, thus revealing their delocalized nature.

Here we introduce an $O(N)$ method of computing the pseudospectrum of large sparse non-Hermitian matrices. The code can be fully parallelized.

For the formulation of our algorithm, we use another definition of the pseudospectrum [4]:

> Definition 2: For any $\varepsilon \geq 0$, the ε-pseudospectrum $\Lambda_\varepsilon(H)$ of a matrix H is the set of the numbers $z \in \mathbf{C}$ satisfying $\sigma_{\min}(z-H) \leq \varepsilon$.

Here $\sigma_{\min}$ denotes the minimum singular value. In other words, the pseudospectrum is the contour plot (with the contour height ε) of the minimum singular value of the non-Hermitian matrix $z - H$ in the complex z plain.

Our new algorithm produces the contour plot by computing the minimum eigenvalue of the Hermitian matrix $\tilde{H} \equiv (z - H)^\dagger (z - H)$, which gives the minimum singular value in the form

$$\sigma_{\min} = \sqrt{\lambda_{\min}\left(\tilde{H}\right)}. \tag{17}$$

The minimum eigenvalue of a large Hermitian matrix is accurately obtained by the Lanczos method, an $O(N)$ method (See Appendix A).

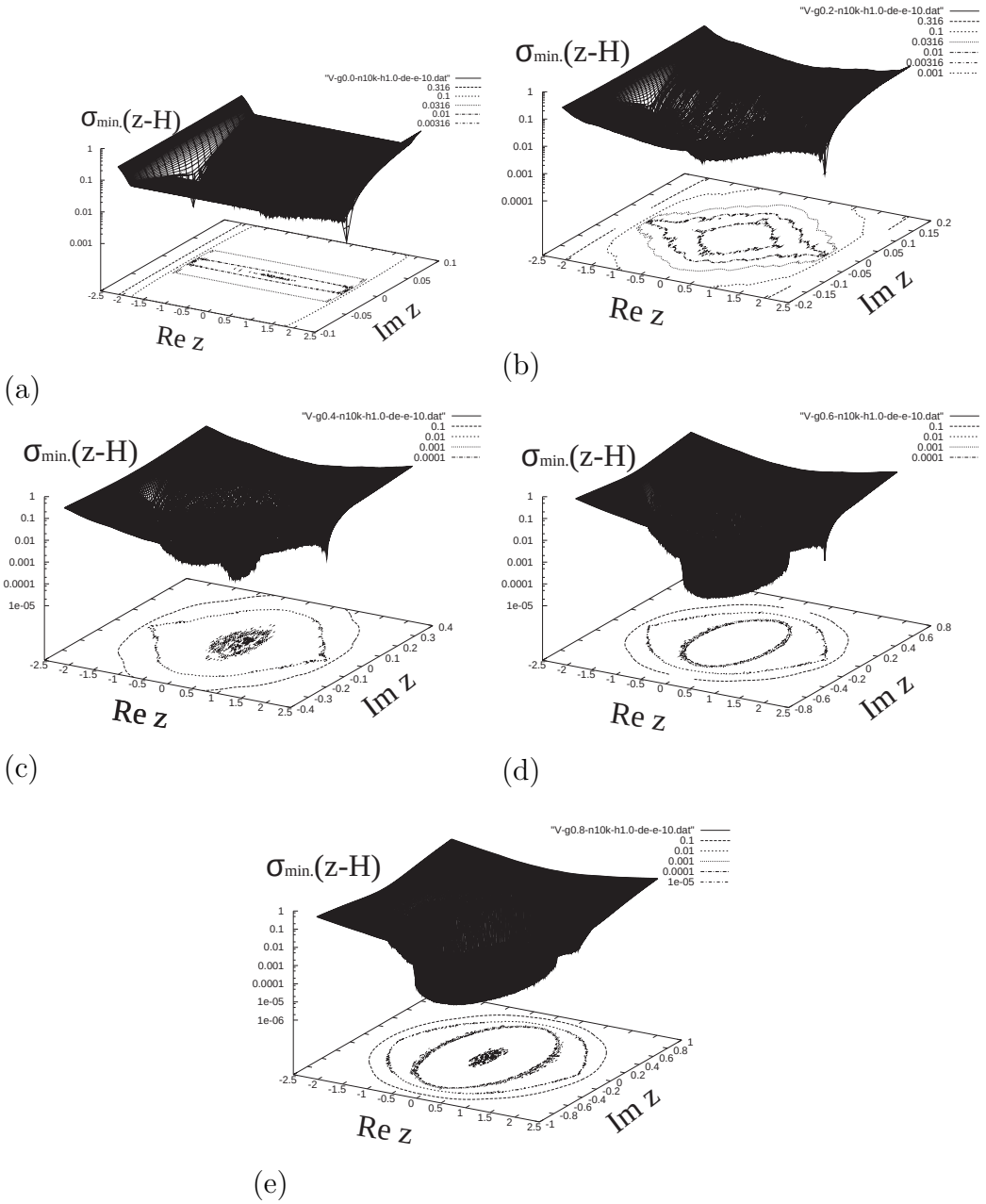

Figure 6: The pseudospectrum $\sigma_{\min}(z-H)$ of the Hamiltonian (9) for various values of g: (a) $g = 0.0$; (b) $g = 0.2$; (c) $g = 0.4$; (d) $g = 0.6$; (e) $g = 0.8$. The system size is $L = 10000$.

4.2 Pseudospectrum of the Anderson Model

Using the above algorithm, we first computed the pseudospctrum of the one-dimentional lattice Anderson Hamiltonian (9). Our numerical results are shown in Fig. 6. The system size is $L = 10000$. We can compare these pseudospectra with the energy spectra in Fig. 1 for $L = 500$.

Let us compare in more details the eigenspectrum and the pseudospectrum. We put together the spectrum and the pseudospectrum for $g = 0.7$ in Fig. 6(a) and Fig. 6(b). In Fig. 6(c) and (d), we superimposed the spectrum and the pseudospectum. In Fig. 6(c), the pseudospectrum has fuzziness of about 0.05 around the mobility edge. In other parts, we see the fuzziness of about 0.02 as shown in Fig. 6(a). In order to suppress the fuzziness, we need to increase the accuracy of the Lanczos method and to make the mesh on the z plain finer.

In plotting the pseudospactrum in Fig. 6(b), we put the contour height $\varepsilon = 0.0092$, since the pseudospectrum with this value approximates the spectrum best for $g = 0.7$. We find that the best value of ε depends on the imaginary vector potential g. As the imaginary vector potential g is increased, we must increase ε to approximate the spectrum best.

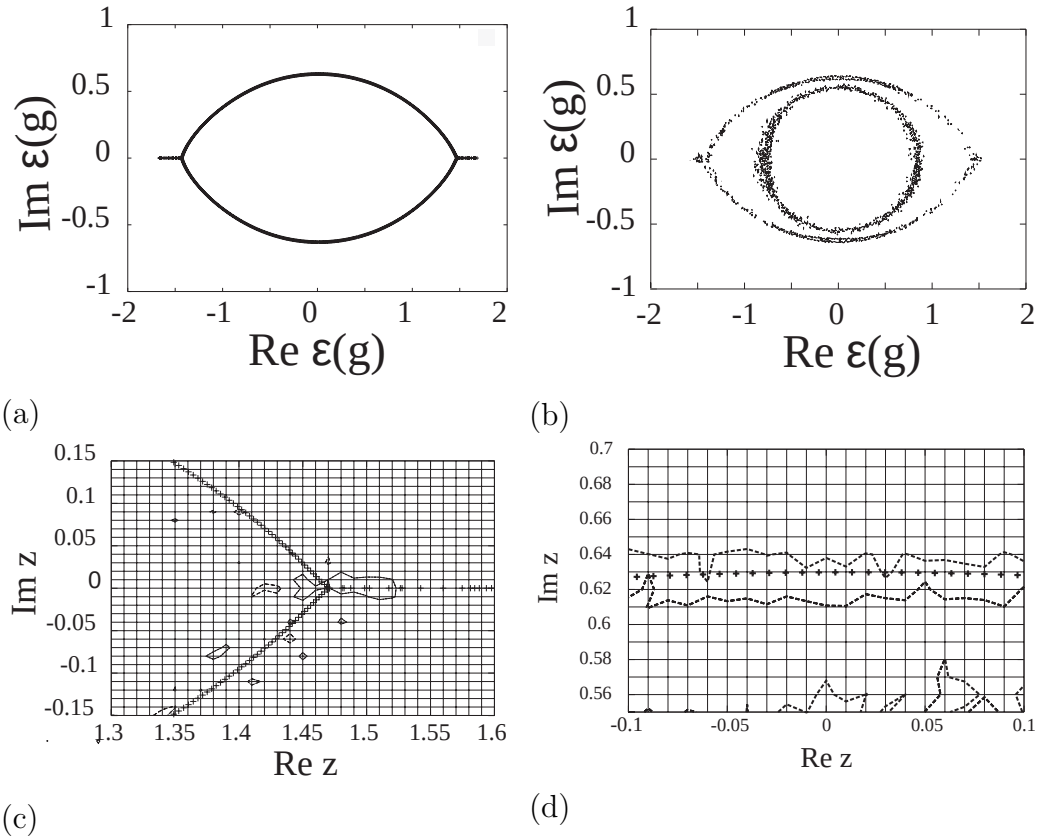

Figure 6: Comparing the eigenspectrum and the pseudospectrum of the Hamiltonian (9) for $g = 0.7$: (a) The eigenspectrum for $g = 0.7$; (b) The pseudospectrum for $g = 0.7$ (the contour plot at $\varepsilon = 0.0092$); (c) A magnified plot of (a) and (b) around the mobility edge; (d) A magnified plot of (a) and (b) near the top of the spectrum. In (c) and (d), the crosses are the eigenvalues and the lines are the contour lines.

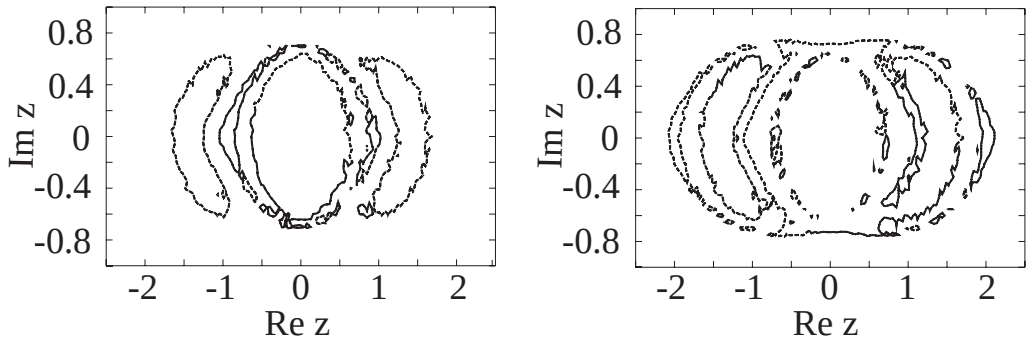

(a) (b)

Figure 7: The contour plot of the pseudospectrum of two-leg the ladder model in a random potential for $g = 0.8$: (a) $\sigma_{\min}(z - H) \leq \varepsilon = 0.0110$; (b) $\varepsilon \leq 0.0155$.

4.3 Pseudo spectrum of the Ladder Models in a Random On-Site Potential

As is shown in Fig. 3, the spectra of the non-Hermitian ladder models are in a random on-site potential N_{leg}fold. The question here is how to observe this structure in the corresponding pseudospectra. We show in Figs. 7–10 the contour plots of the pseudospectrum with the contour height ε varied. In each figure, there is one value of ε for which we can see an approximate shape of the energy spectrum.

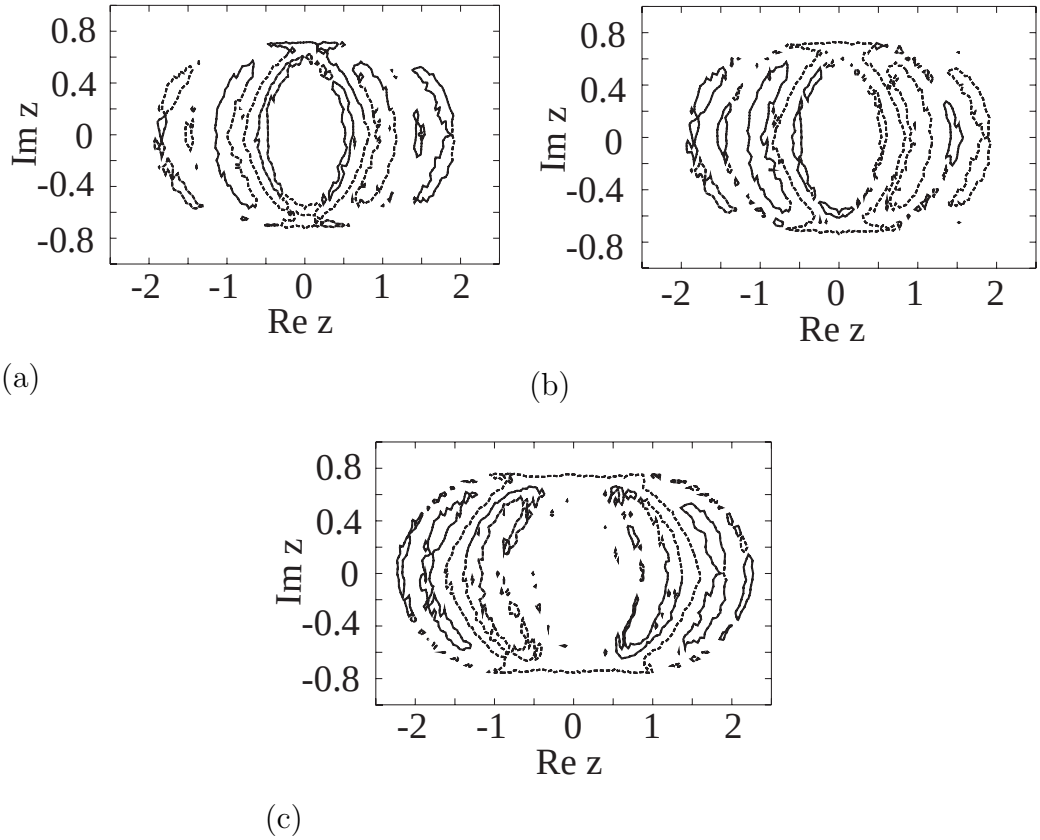

Figure 8: The contour plot of the pseudospectrum of the three-leg ladder model in a random potential for $g = 0.8$. (a) $\sigma_{\min}(z - H) \leq \varepsilon = 0.0124$; (b) $\varepsilon = 0.0135$; (c) $\varepsilon = 0.0165$.

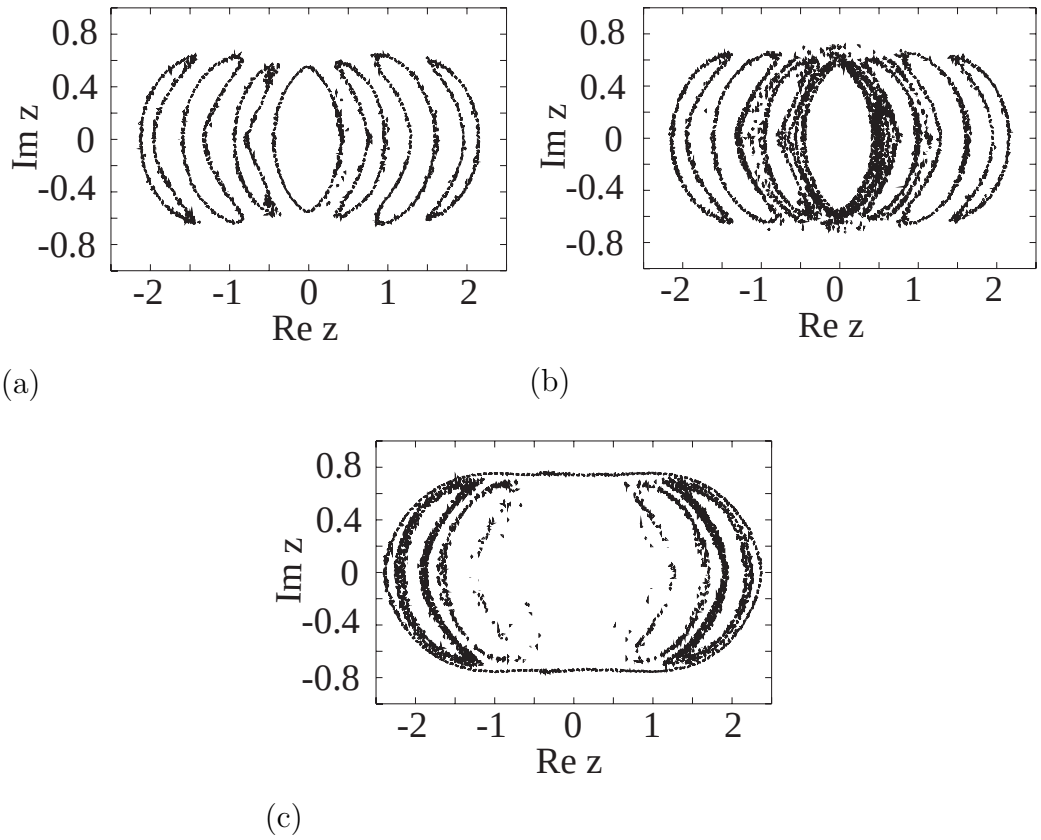

Figure 9: The contour plot of the pseudospectrum of the four-leg ladder model in a random potential for $g = 0.8$. (a) $\sigma_{\min}(z - H) \leq \varepsilon = 0.0020$; (b) $\varepsilon = 0.0035$; (c) $\varepsilon = 0.0080$.

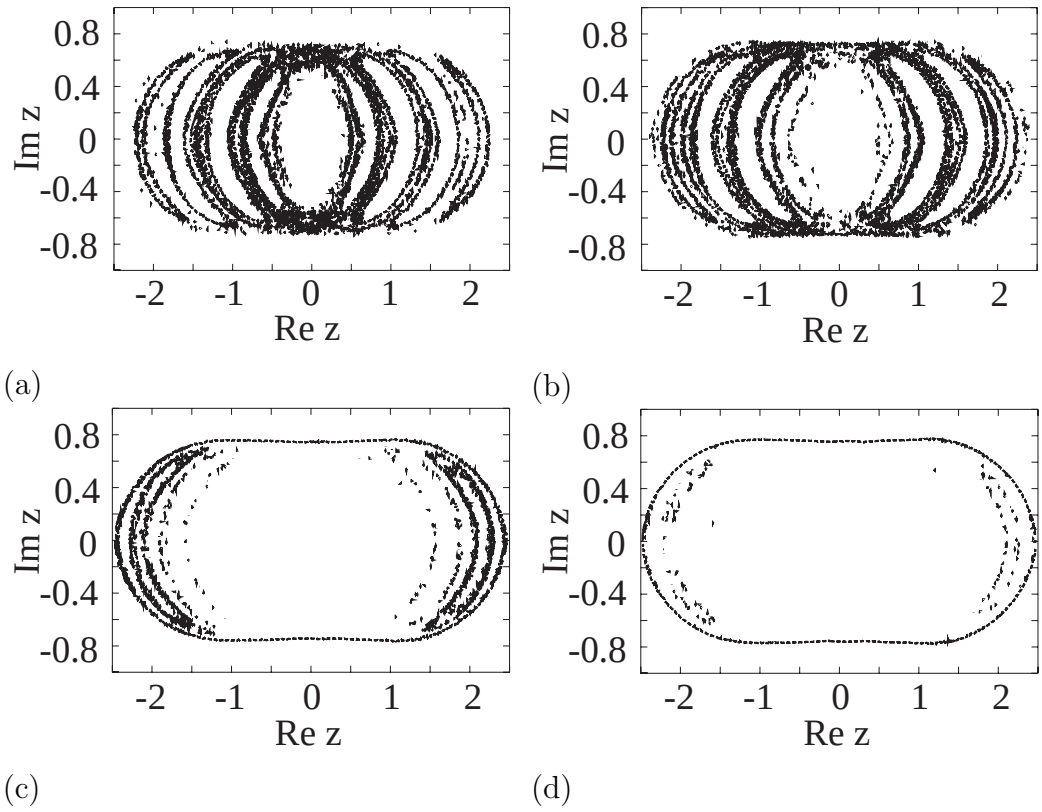

Figure 10: The contour plot of the pseudospectrum of the five-leg ladder model in a random potential for $g = 0.8$. (a) $\sigma_{\min}(z - H) \leq \varepsilon = 0.004$; (b) $\varepsilon = 0.005$; (c) $\varepsilon = 0.010$; (d) $\varepsilon = 0.015$.

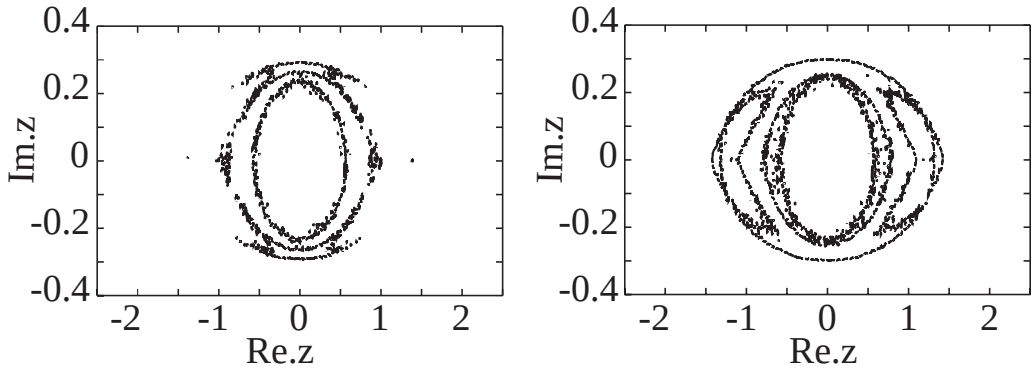

(a) (b)

Figure 11: The contour plot of the pseudospectrum of two-leg the ladder model in a random flux for $g = 0.4$: (a) $\sigma_{\min}(z - H) \leq \varepsilon = 0.0079$; (b) $\varepsilon \leq 0.0099$;

4.4 Pseudospectrum of the Ladder Models in a Random Magnetic Field

As is shown in Figs. 4 and 5, the spectra of the non-Hermitian ladder models in a random magneticfield are N_{leg}-fold. We show in Figs. 11–14 the same plots as in Figs. 7-10 but for the random-field model. From these results, we find in this model, that the closer to the band center a branch of the spectrum is, the lower the contour height ε must be.

In Fig. 14, the inner structure of the pseudospectrum is quite fuzzy. This is presumably because the ladder length is as small as $L = 2000$. We have to compute larger matrices to see the pseudospectrum more accurately.

Unfortunately, to date, we could not analyze the psuedospectrum accurately. We expect, however, that the psuedospectrum is useful in analyzing the energy spectrum of large non-Hermitian matrices, and thereby in estimating the localization length of the Hermitian Anderson model.

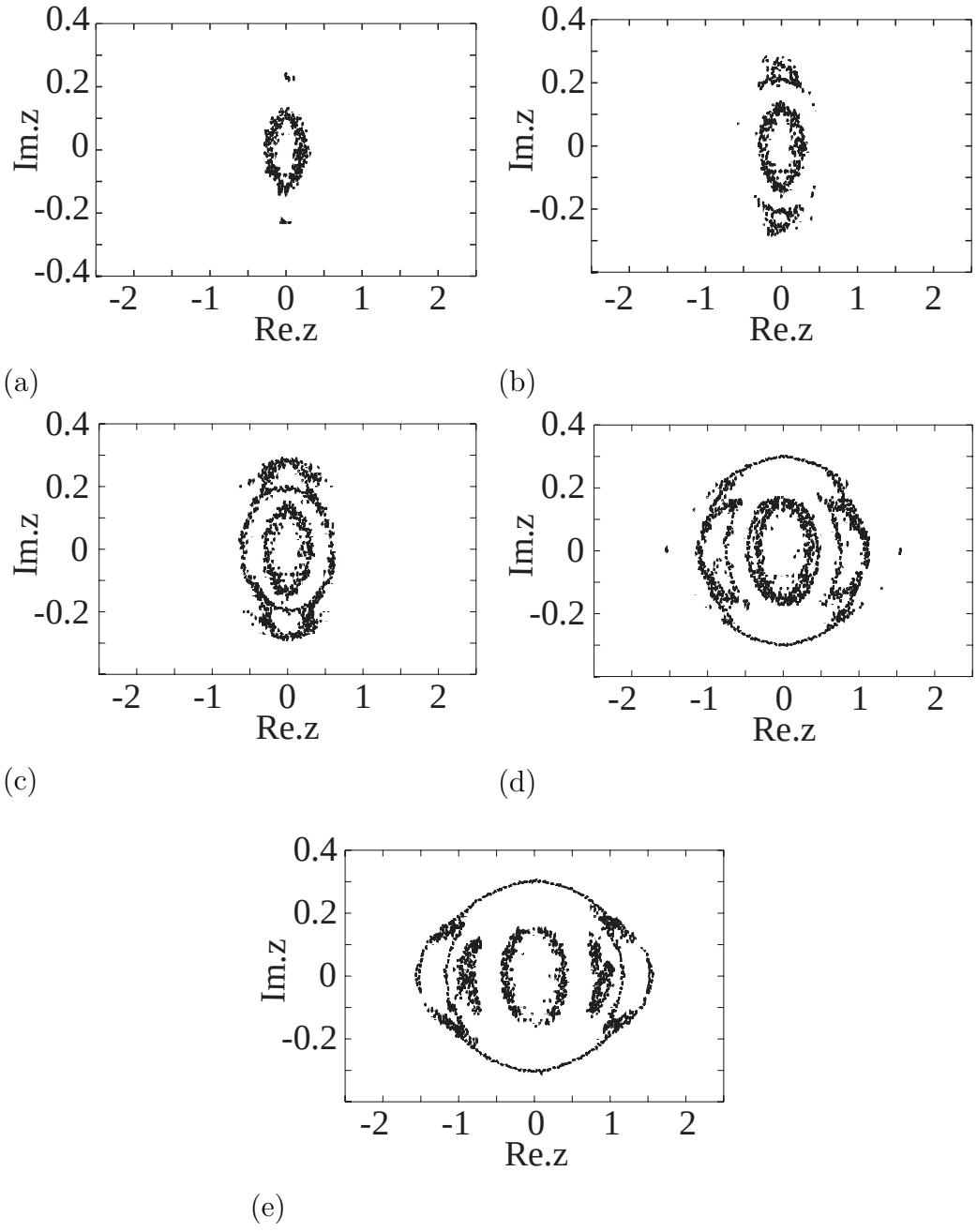

Figure 12: The contour plot of the pseudospectrum of the three-leg ladder model in a random flux for $g = 0.4$. (a) $\sigma_{\min}(z - H) \leq \varepsilon = 0.0058$; (b) $\varepsilon = 0.0069$; (c) $\varepsilon = 0.0077$; (d) $\varepsilon = 0.0100$; (e) $\varepsilon = 0.0112$.

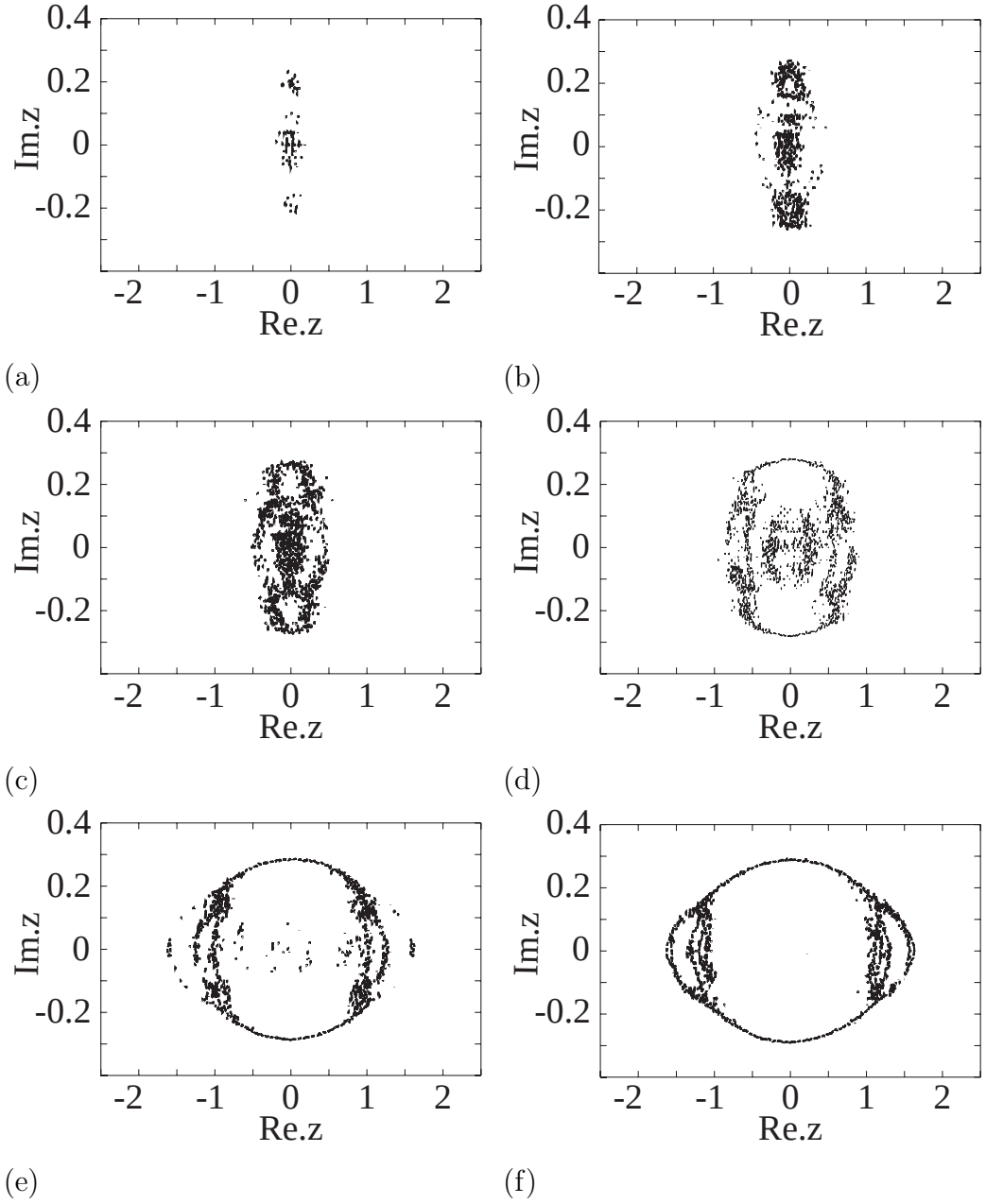

Figure 13: The contour plot of the pseudospectrum of the four-leg ladder model in a random flux for $g = 0.4$. (a) $\sigma_{\min}(z - H) \leq \varepsilon = 0.0062$; (b) $\varepsilon = 0.0070$; (c) $\varepsilon = 0.0076$; (d) $\varepsilon = 0.0092$; (e) $\varepsilon = 0.0108$; (f) $\varepsilon = 0.0117$.

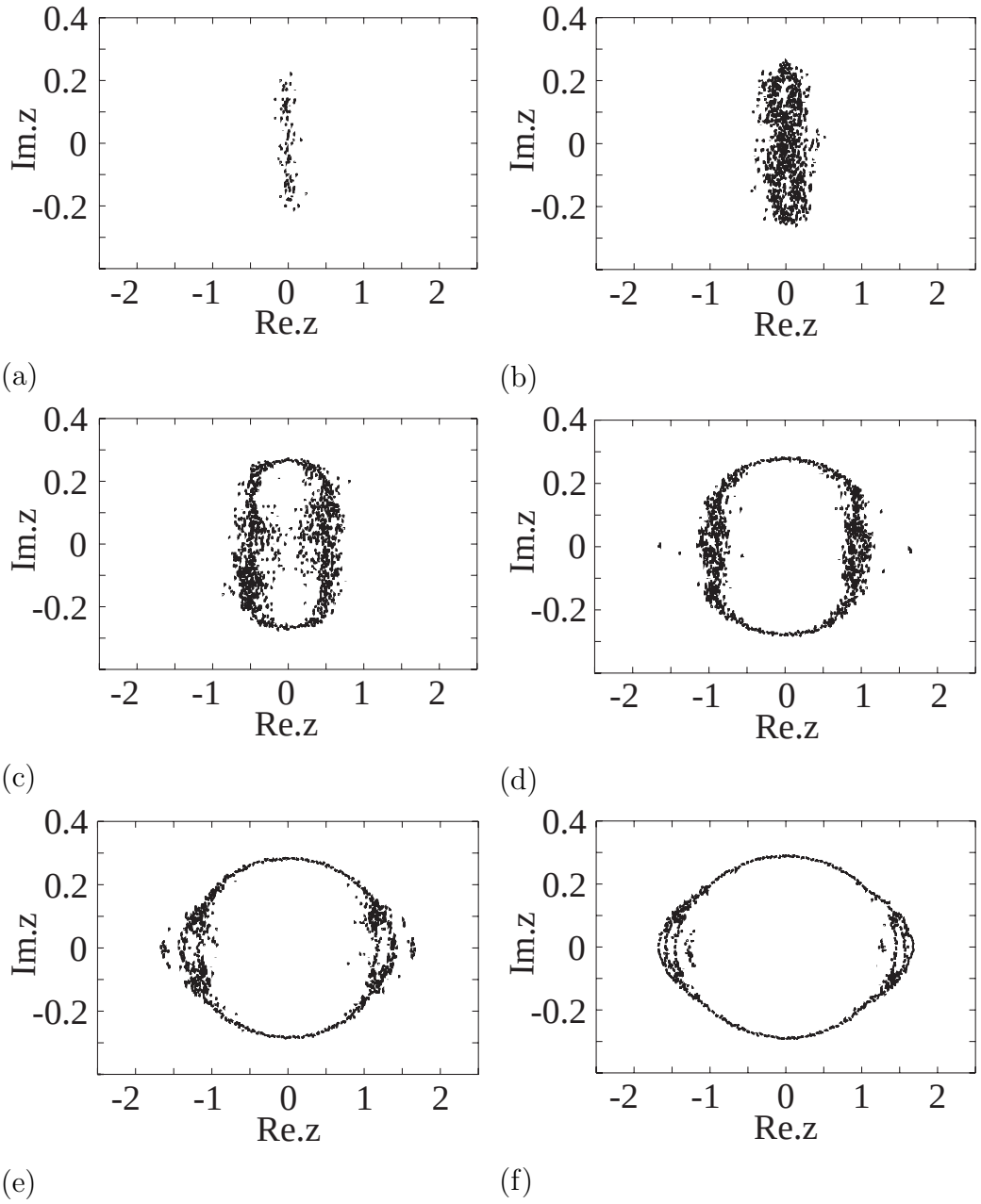

Figure 14: The contour plot of the pseudospectrum of the five-leg ladder model in a random flux for $g = 0.4$. (a) $\sigma_{\min}(z - H) \leq \varepsilon = 0.0062$; (b) $\varepsilon = 0.0072$; (c) $\varepsilon = 0.0087$; (d) $\varepsilon = 0.0105$; (e) $\varepsilon = 0.0116$; (f) $\varepsilon = 0.0132$.

5 Summary

We studied various Anderson models in one dimension by using the technique of the non-Hermitian Hamiltonian. We can compute the inverse localization length κ directry from the eigenspectrum of non-Hermitian Hamiltonian. However, it is difficult to compute the eigenspectrum of large non-Hermitian matrices. Hence we proposed the new algorithm of computing the pseudospectrum which approximates the eigenspectrum of non-Hermitian Hamiltonian. We thereby observed the difference between the eigenspectrum of the model in a random on-site potential and the model in a random flux.

Acknowledgements

The author is grateful to Prof. N.Hatano for help.

A Lanczos Method

In the present study, we diagonalize Hermitian matrices to compute the minimum singular value of non-Hermitian matrices. In this Appendix, we explain the Lanczos method of tridiagonalizing Hermitian matrices, which we use in the process of the diagonalization. It is relatively difficulut to diagonalize a matrix directly, so that we tridiagonalize it first. It is much easier to diagonalize the matrix that was tridiagonalized by the Lanczos method.

The Lanczos method involves partial tridiagonalizations of a given Hermitian matrix A. The full submatrices are eventually generated. However, information about the extremal eigenvalues of A tends to emerge long begore the tridiagonalization is complete. This makes the Lanczos algorithm particularly useful in situations where a few of the largest or smallest eigenvalues of A are desired.

Consider an $N \times N$ Hermitian matrix A. We tridiagonalize it using some $O(N)$ vectors. We suppose that the matrix A is tridiagonalized to the matrix

$$T_k = \begin{pmatrix} \alpha_1 & \beta_1 & 0 & 0 & 0 \\ \beta_1 & \alpha_2 & \beta_2 & 0 & 0 \\ 0 & \beta_2 & \ddots & \ddots & 0 \\ 0 & 0 & \ddots & \alpha_{k-1} & \beta_{k-1} \\ 0 & 0 & 0 & \beta_{k-1} & \alpha_k \end{pmatrix}, \tag{18}$$

using a matrix Q_k,

$$Q_k^\dagger A Q_k = T_k, \tag{19}$$

where Q_k is given by

$$Q_k = (\vec{q_1}\vec{q_2}\vec{q_3}\cdots\vec{q_k}) \tag{20}$$

with an orthonormal set of vectors

$$\vec{q_i}^\dagger \vec{q_i} = \delta_{ij}. \tag{21}$$

From Eq. (19), we have

$$AQ_k = Q_k T_k. \tag{22}$$

Thus we find

$$A\vec{q_i} = \beta_{i-1}\vec{q}_{i-1} + \alpha_i \vec{q_i} + \beta_i \vec{q}_{i+1}, \tag{23}$$

or

$$\vec{q}_{i+1} = \frac{1}{\beta_i}\left(A\vec{q_i} - \beta_{i-1}\vec{q}_{i-1} - \alpha_i\vec{q_i}\right). \tag{24}$$

We notice that we can generate the vector $\vec{q}_{i+1}$ from the vectors $\vec{q}_{i-1}$ and $\vec{q}_i$, simply by multiplying the matrix A to the vector $\vec{q}_i$. This is an $O(N)$ operation, which is the key point of the Lanczos method.

The computation of the tridiagonal matrix T_k proceeds as follows. First, we compute the diagonal elements α_k from (23) as

$$\begin{aligned} \vec{q}_i^{\dagger} A \vec{q}_i &= \beta_{i-1} \vec{q}_i^{\dagger} \vec{q}_{i-1} + \alpha_i \vec{q}_i^{\dagger} \vec{q}_i + \beta_i \vec{q}_i^{\dagger} \vec{q}_{i+1} \\ &= \alpha_i, \end{aligned} \tag{25}$$

since we have the orthogonomality $\vec{q}_i^{\dagger} \vec{q}_{i-1} = 0, \quad \vec{q}_i^{\dagger} \vec{q}_i = 1, \quad \vec{q}_i^{\dagger} \vec{q}_{i+1} = 0.$ Thereby, we have

$$\alpha_i = \vec{q}_i^{\dagger} A \vec{q}_i \tag{26}$$

Second, the vector (24) must be a unit vector:

$$1 = |\vec{q}_{i+1}| = \frac{1}{\beta_i} |A\vec{q}_i - \vec{\beta}_{i-1} \vec{q}_{i-1} - \alpha_i \vec{q}_i|. \tag{27}$$

Thus we can compute the subdiagonal factors β_k as

$$\beta_i = |A\vec{q}_i - \beta_{i-1} \vec{q}_{i-1} - \alpha_i \vec{q}_i|. \tag{28}$$

Computing the elements α_i and β_i one by one, we can construct the tridiagonalized matrix (18).

References

[1] N. Hatano and D.R. Nelson, Phys. Rev. Lett. **77** (1996) 570; Phys. Rev. B **56** (1997) 8651; Phys. Rev. B **58** (1998) 8384.

[2] N. Hatano: Physica A **254** (1998) 317.

[3] L.N. Trefthen, Acta Numerica **8** (1999) 247.

[4] L.N. Trefthen, M. Contedini, and M. Embree, preprint.

[5] J. T. Edwards and D. J. Thouless, J. Phys. C **5**, 807 (1972).

[6] D. J. Thouless, Phys. Rep. **13** (1974) 93; Phys. Rev. Lett. **39** (1975) 1167.

[7] D. C. Liccardello and D. J. Thouless, J. Phys. C **8**, 4157 (1975).